Iranian Journal of Catalysis 9(1), 2019, 27-35

IRANIAN JOURNAL OF CATALYSIS

Green synthesis of $Ag/Fe_3O_4/ZrO_2$ nanocomposite using aqueous *Centaurea cyanus* flower extract and its catalytic application for reduction of organic pollutants

Akbar Rostami-Vartooni[a,*], Abolfazl Moradi-Saadatmand[a], Mojtaba Bagherzadeh[b], Mohammad Mahdavi[c]

[a]*Department of Chemistry, Faculty of Science, University of Qom, Qom 3716146611, Iran.*

[b]*Reactor and Nuclear Safety School, Nuclear Science and Technology Research Institute, 81465-1589, Isfahan, Iran.*

[c]*Department of Chemistry, Malek-ashtar University of Technology, Shahin-shahr P.O. Box 83145/115, Iran.*

Received 30 July 2018; received in revised form 12 October 2018; accepted 15 October 2018

ABSTRACT

In this work, at first, nano ZrO_2 and Fe_3O_4/ZrO_2 nanocomposite were prepared by sol-gel and co-precipitation methods, respectively. Then, Ag nanoparticles (Ag NPs) were mixed with them in environmentally friendly and mild conditions using *C. cyanus* flower extract as a reducing and stabilizing agent. The synthesized nanocomposites were characterized by FT-IR, XRD, FE-SEM, EDS, and VSM techniques. The experimental results confirmed formation of the Ag nanoparticles with the 30-90 nm diameter on the surface of supports at room temperature within a few minutes. After that, the catalytic activity of the prepared nanocomposites in reduction of 4-nitrophenol (4-NP) and methyl orange (MO) have been studied and our results showed that they have following sequence: Ag/ZrO_2 > $Ag/Fe_3O_4/ZrO_2$ > ZrO_2 > ZrO_2 (550 °C) > Fe_3O_4/ZrO_2. Finally, the magnetically recoverable $Ag/Fe_3O_4/ZrO_2$ nanocomposite could be reused three times without a considerable decrease in its catalytic activity. Observed results were presented here and the probable catalytic mechanism was discussed.

Keywords: *Centaurea cyanus, Ag nanoparticles, Zirconia, Magnetic support, Green synthesis, Organic pollutant.*

1. Introduction

The removal of organic pollutants from wastewater is one of the most problems of human living system [1-6]. A number of practical techniques such as advanced oxidation processes (AOPs), biological degradation and adsorption have been reported to remove these contaminants [7-15]. In current decade, the reduction process, in the presence of $NaBH_4$ and metal nanoparticles (MNPs) or nanocomposites, is reported as an effective method for the elimination of toxic nitroarene compounds and azo dyes from water [16,17]. Consequently, development of different physical and chemical methods for synthesis of the MNPs with large surface area attracted considerable attention in recent years due to their higher reactivity in comparison to the particulate metal counterpart [18,19].

*Corresponding author.
E-mail addresses: a.rostami@qom.ac.ir, a.rostami127@yahoo.com (A. Rostami-Vartooni)

Between them, the application of aqueous extract of the plants, as nontoxic reducing and stabilizing agents, is a new technique for green synthesis of the MNPs under mild conditions [20,21].

However, immobilization of the MNPs on a supports surface, significantly decreases their agglomeration, this also causes to increase the catalytic activity of nanoparticles and simplify their separation process. Recently both organic supports like biowasts and inorganic supports such as bentonite, zeolite, silica, alumina and metal oxides have been used extensively for immobilization of the MNPs on their surface [22,23]. Zirconia (ZrO_2) as an inorganic oxide possesses unique properties such as a chemical inertness, suitable thermal stability, and good mechanical, electrical and optical properties and it has been widely used as a support, catalyst, photocatalyst, etc. [24,25]. Herein, first, nano ZrO_2 and Fe_3O_4/ZrO_2 nanocomposite were prepared by sol-gel and co-precipitation methods, respectively. These nanocomposites were prepared as

supports for immobilization of Ag nanoparticles (Ag NPs). The Ag NPs were immobilized on the prepared supports in environmentally friendly and mild conditions using the cornflower extract as a reducing and stabilizing agent to prepare Ag/ZrO_2 and $Ag/Fe_3O_4/ZrO_2$ nanocomposites.

Cornflower (*Centaurea cyanus*) as a beneficial weed and well-known herbal medicine has both tonic and stimulant properties. This plant was historically used for its blue pigment (protocyanin). *C. cyanus* in treating conjunctivitis, for washing of tried eyes and as an ingredient in herbal bags. The antioxidant, antitumor and antibacterial activities of this plant extract are contributed to the presence of the phytochemical constituents such as n-hexadecanoic acid and linoleic acid [26,27]. Based on our literature survey, there is no report on the biosynthesis of metal nanocomposites using *C. cyanus* extract. Prepared nanocomposites were characterized using physical and chemical methods such as FT-IR, XRD, FE-SEM, EDS, and VSM techniques. Finally, the catalytic reduction of two organic pollutants (4-NP and MO) was carried out with ZrO_2, Fe_3O_4/ZrO_2, Ag/ZrO_2, and $Ag/Fe_3O_4/ZrO_2$ nanocomposites. The observed results and probable catalytic mechanism are presented and discussed here.

2. Experimental

2.1. Chemical substances and instruments

All chemical substances used in this work were obtained from Merck KGaA, Darmstadt, Germany. The *C. cyanus* plant was collected from the Isfahan Province, Iran (Vartoon village). Fourier transform infrared (FT-IR) spectra were recorded on a Nicolet 370 FT/IR spectrometer (Thermo Nicolet, USA) using KBr pellets. For the phase identification and characterization of crystal structure of the prepared nanocomposites, a Philips PW3040 X-ray diffractometer (Cu Kα = 1.5405 Å) was used. Spectrophotometric absorption measurements in the wavelength ranges of 200–750 nm was carried out on a double-beam spectrophotometer (Hitachi, U-2900). FE-scanning electron microscopy (FE-SEM) is another commonly used method of characterization which was performed on a Cam scan MV2300. Energy-dispersive X-ray spectroscopy (EDS) was used for evaluation of the chemical composition of the prepared ZrO_2 nanocomposites. Vibrating sample magnetometer (VSM) measurement was measured using a SQUID magnetometer at 298 K (Quantum Design MPMS XL) in the magnetic field intensity (H) range of –8500 to +8500 Oe.

2.2. Preparation of extract

15 g of dried flowers of *C. cyanus* plant was mixed in 100 mL distilled water and heated at 60 °C for 25 min. Afterwards, the filtered extract was used for reduction of Ag^+ ions to Ag NPs on the surface of supports.

2.3. Preparation of ZrO_2 NPs

A solution of 0.3 mL distilled water and 0.3 mL HCl (37% w/w) was added dropwise to a homogeneous mixture of 2 g $ZrCl_4$ and 5 mL n-propanol under vigorous stirring and refluxed at 80 °C for 2 h. Then, the pH of resulted $Zr(OPr)_4$ solution was adjusted to 8 by addition of 1.5 M NaOH solution. Finally, the produced ZrO_2 NPs was washed with distilled water and dried in a furnace at 80 °C.

2.4. Preparation of Fe_3O_4/ZrO_2 nanocomposite

A solution of 5.2 g $FeCl_3$ and 2 g $FeCl_2$ in 25 mL HCl (1 M) was degassed with N_2 gas for 15 min and added dropwise into the vigorous stirred NaOH solution (250 mL, 1.5 M) at 80 °C. The prepared Fe_3O_4 nanoparticles were separated from the solution and washed with water four times. The resulting Fe_3O_4 nanoparticles was added into the freshly prepared solution of 1.0 M in $ZrCl_4$ and 0.23 M in $HClO_4$, and the pH value of the mixture was adjusted to 8.0 by addition of 2 M NaOH within 1 h. Finally, the formed Fe_3O_4/ZrO_2 NPs (2 : 5 w/w) were washed with distilled water and dried in an oven at 80 °C [28].

2.5. Preparation of Ag/ZrO_2 nanocomposite

A solution of 0.1 M $AgNO_3$ (25 mL) was added to a mixture of 2 g ZrO_2 NPs dispersed in 50 mL of the *C. cyanus* flower extract. This mixture was stirred for 15 min at room temperature until the white color of the ZrO_2 NPs changes to dark color, indicating the formation of Ag NPs on its surface. Finally, the prepared Ag/ZrO_2 nanocomposite was filtered and washed with distilled water.

2.6. Preparation of $Ag/Fe_3O_4/ZrO_2$ nanocomposite

2.0 g Fe_3O_4/ZrO_2 was dispersed in the 50 mL of the prepared *C. cyanus* extract under stirring. Then, 25 mL of $AgNO_3$ solution (0.1 M) was added to this mixture and stirred at room temperature for 15 min under continuous stirring. Finally, the produced $Ag/Fe_3O_4/ZrO_2$ was filtered and washed with distilled water.

2.7. Reduction of MO and 4-NP by ZrO_2 nanocomposites

The catalytic reduction of MO and 4-NP as organic pollutants was carried out using as-prepared ZrO_2

nanocomposites. Typically, freshly prepared $NaBH_4$ solution (30 mL, 5.3×10^{-3} M) was added to a solution that contained MO (30 mL, 3×10^{-5} M) and different amounts of the ZrO_2 nanocomposites as catalysts. Then, the mixture was stirred at room temperature and the reduction process was monitored by UV–Vis absorption analysis at certain intervals. In the reduction process of 4-NP, 30 mL of freshly prepared $NaBH_4$ solution (4.4×10^{-2} M) was added to 30 mL of 4-NP solution (2.5×10^{-3} M) in the presence of 3 or 6 mg catalysts at room temperature.

3. Results and Discussion

3.1. Characterization of C. cyanus extract

The presence of organic compounds with hydroxyl and carbonyl functional groups in the flower of *C. cyanus* plant as reducing and stabilizing agents are confirmed by FT-IR and UV-Vis techniques. The phenolic constituents in the flower of *C. cyanus* show a broad absorption band at 3380 cm^{-1} and some absorptions at 1030-1335 cm^{-1} in FT-IR spectrum (Fig. 1a) [29,30]. Also, CH_3 or CH_2 units, C=C and C=O bands show the absorption signals at about 2927, 1635-1735 and 1420 cm^{-1}, respectively [31,32]. The maximum absorption bands at 267 and 336 nm in the UV-Vis spectrum of *C. cyanus* flower extract (Fig. 1b) are assigned to $\pi \rightarrow \pi^*$ and $n \rightarrow \pi^*$ transitions which can be related to the presence of C=O and C=C bonds.

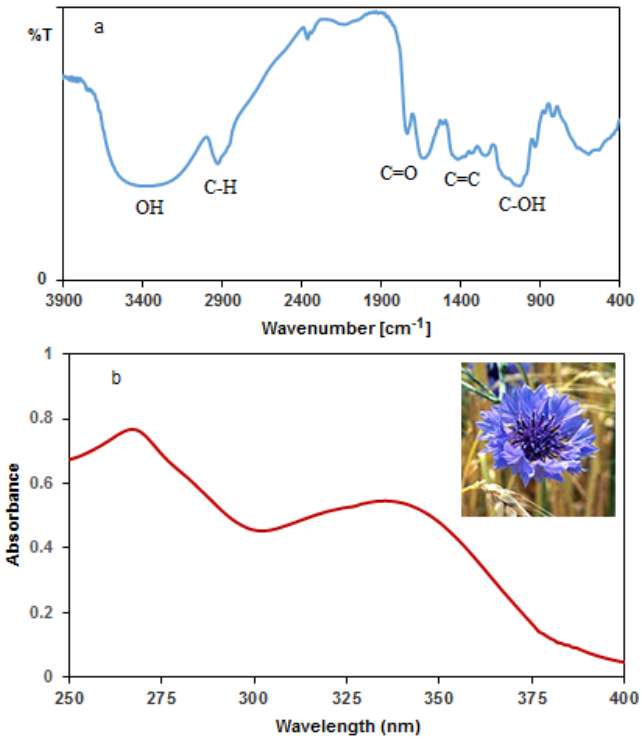

Fig. 1. FT-IR (a) and UV-Vis (b) spectra of *C. cyanus*.

3.2. Characterization of nano zirconia and its nanocomposites

FT-IR spectra obtained for the ZrO_2 NPs and its nanocomposites have been shown in Fig. 2. The absorption bands at about 450-750 cm^{-1}, 1300-1400 cm^{-1} and 1550-1650 cm^{-1} are related to the Zr–O–Zr, Zr–O and Zr–OH bonds, respectively [33-36]. Fe–O vibrations are appeared at the range of 430-700 cm^{-1} for Fe_3O_4 nanocomposites [37,38]. A broad peak has produced at the range of 3426-3450 cm^{-1} by the stretching vibration of OH groups on the surface of ZrO_2 nanocomposites [39]. According to this figure, the functional groups on nano ZrO_2 and Fe_3O_4/ZrO_2 nanocomposite have not changed after the immobilization of Ag NPs.

The XRD patterns obtained for the nano zirconia and its nanocomposites have been shown in Fig. 3.

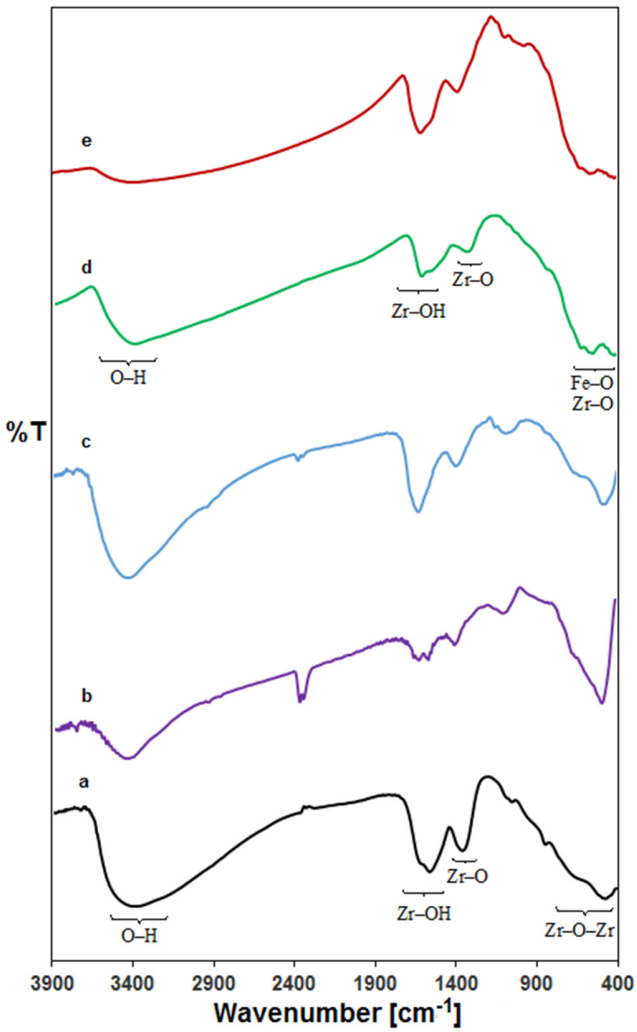

Fig. 2. FT-IR spectra of as-prepared ZrO_2 NPs (a), ZrO_2 NPs annealed at 550 °C (b), Ag/ZrO_2 (c) Fe_3O_4/ZrO_2 (d) and $Ag/Fe_3O_4/ZrO_2$ (e).

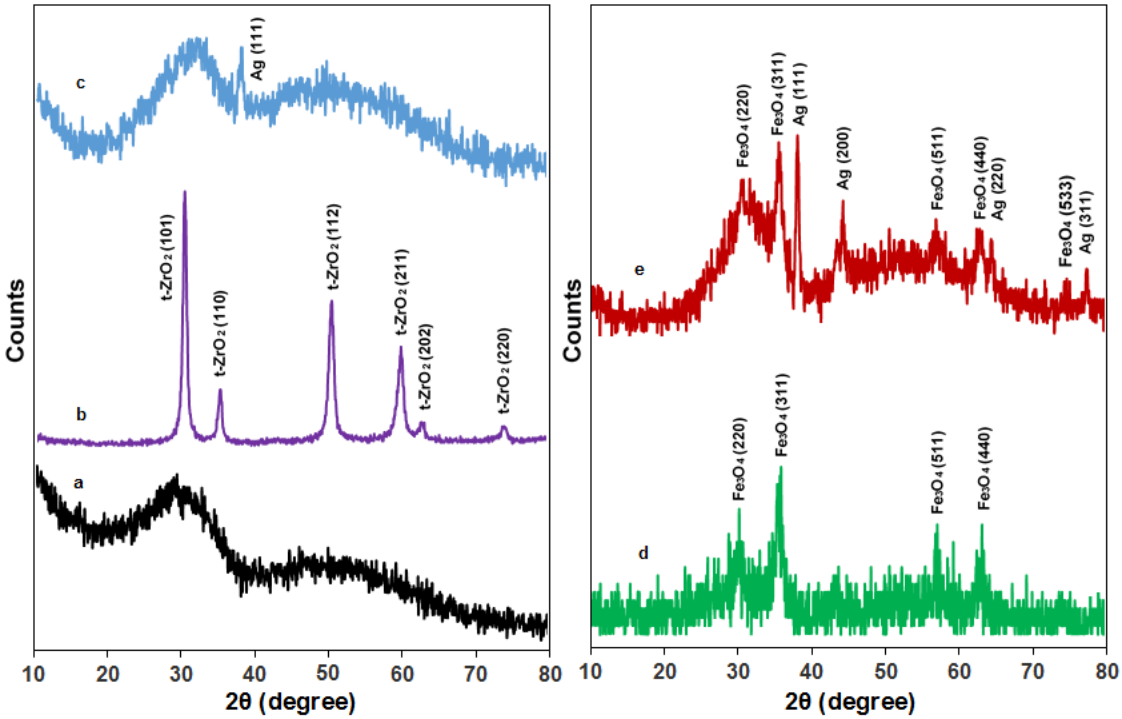

Fig. 3. XRD patterns of as-prepared ZrO_2 NPs (a), ZrO_2 NPs annealed at 550 °C (b), Ag/ZrO_2 (c) Fe_3O_4/ZrO_2 (d) and Ag/Fe_3O_4/ZrO_2 (e).

It is clear that the as-prepared ZrO_2 NPs indicates amorphous nature whereas its calcined form (at 550 °C) is in the crystalline state which shows the diffraction peaks at 30.5°, 35.4°, 50.7°, 60.3°, 63.5° and 74.5° relating to the (101), (110), (112), (211), (202) and (220) reflections of tetragonal phase of zirconia nanoparticles, respectively [40-43]. The characteristic peaks at about 2θ = 30.8°, 35.9°, 57.3° and 63.1° in the XRD patterns of Fe_3O_4/ZrO_2 and Ag/Fe_3O_4/ZrO_2 nanocomposites (Figs. 3d and 3e) are related to the (220), (311), (511) and (440) planes of the cubic spinel phase of the magnetite compound [44,45]. The formation of Ag NPs is approved by characteristic peaks in the XRD patterns of Ag nanocomposites (Figs. 3c and 3e) at about 2θ = 38.3°, 44.3°, 64.7° and 77.6° corresponding to the (111), (200), (220) and (311) reflections [46,47]. The average crystallite sizes of Ag NPs on ZrO_2 NPs, ZrO_2(550) and Fe_3O_4/ZrO_2 which are estimated using the Debye Scherrer equation [48,49] are about 22, 40 and 45 nm, respectively.

The morphology of the as-prepared nano ZrO_2, Ag/ZrO_2 and Ag/Fe_3O_4/ZrO_2 were investigated by FE-SEM (Figs. 4 and 5). As can be seen in these figures, the spherical Ag NPs with 30-90 nm diameter were immobilized on the surface of as-prepared ZrO_2 NPs and its Fe_3O_4 nanocomposite. The particle size distributions of AgNPs are found to be close to the average grain sizes calculated by the Debye Scherrer equation. The presence of Zr, O, Ag or Fe elements in Ag/ZrO_2 and Ag/Fe_3O_4/ZrO_2 were confirmed by EDS (Fig. 6).

To evaluate the magnetic properties of Ag/Fe_3O_4/ZrO_2 nanocomposite, the VSM magnetization curve was applied. The hysteresis loop obtained using a magnetometer at 298 K is shown in Fig. 7. The saturation magnetization (Ms) value of this nanocomposite at saturation point of the hysteresis loop was about 10 $emug^{-1}$. The hysteresis loop confirms the soft magnetic nature of the synthesized nanocomposite which can be simply magnetized and demagnetized. The Ag/Fe_3O_4/ZrO_2 has the paramagnetic behavior and its Ms value is enough for magnetic separation of nanocomposite from the reaction mixture by applying an external magnetic field.

3.3. Catalytic ability evaluation of ZrO_2 NPs and its nanocomposites

In this work, the reduction process of MO and 4-NP in the presence of $NaBH_4$ were evaluated using ZrO_2 NPs and its Fe_3O_4 nanocomposite before and after immobilization of Ag NPs. As depicted in Fig. 8, the intensity of UV–Vis bands at 493 and 400 nm disappeared within 7.5 and 9 min for aqueous solutions of MO (3×10^{-5} M, 30 mL) and 4-NP (2.5×10^{-3} M, 30 mL), respectively. With disappearance of the peak at 400 nm in UV–Vis spectrum of 4-NP, a new peak at

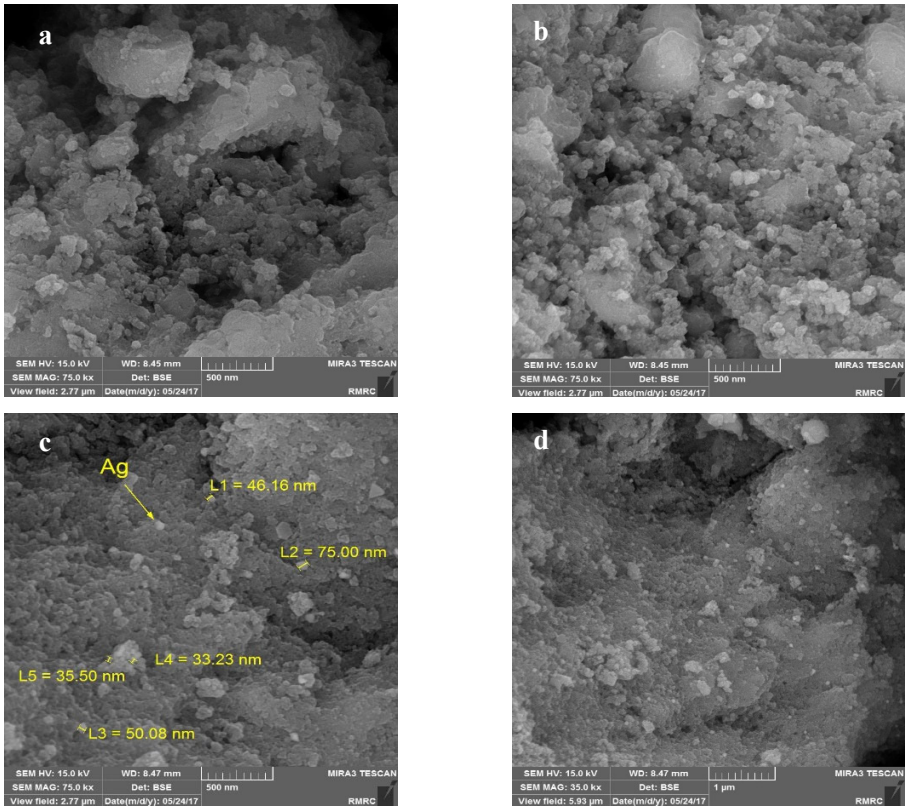

Fig. 4. FE-SEM images of as-prepared ZrO_2 NPs (a and b) and and its Ag nanocomposite (c and d).

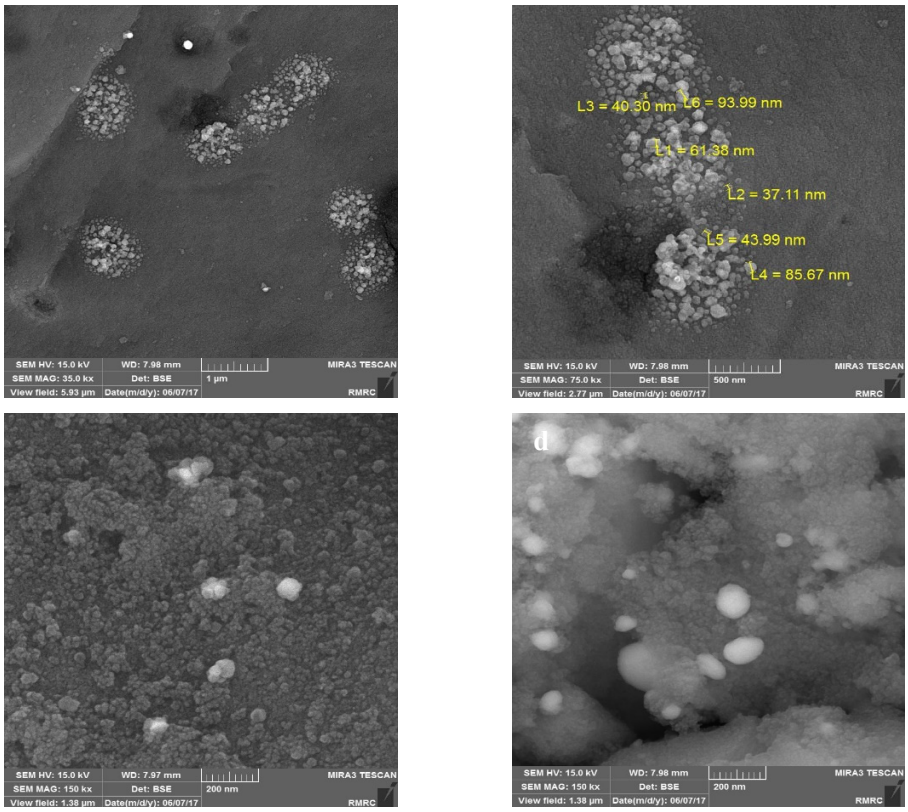

Fig. 5. FE-SEM images of $Ag/Fe_3O_4/ZrO_2$ nanocomposite.

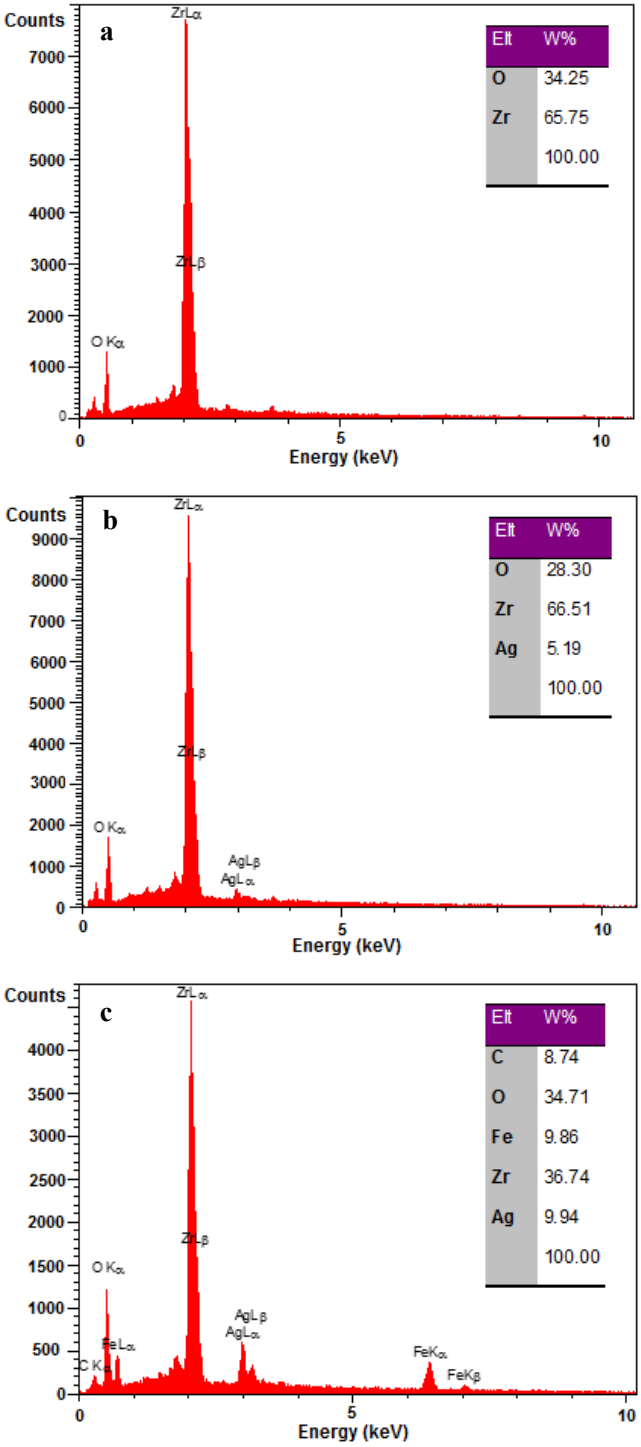

Fig. 6. EDS spectra of as-prepared ZrO_2 NPs (a), Ag/ZrO_2 (b) and Ag/Fe_3O_4/ZrO_2 (c).

about 300 nm appeared, this clearly indicated the formation of 4-aminophenol [50]. Table 1 shows the complete reduction times of MO and 4-NP in different conditions. Without any catalyst and $NaBH_4$, the reduction performance was slow. The addition of higher amount of the catalysts and $NaBH_4$ leads to the higher increase in reduction of selected organic dyes.

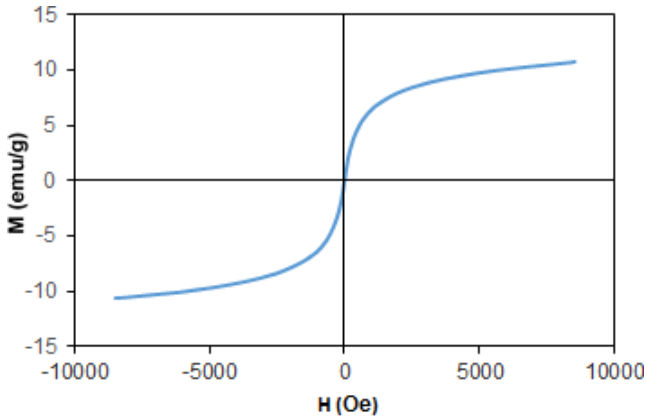

Fig. 7. Typical VSM of Ag/Fe_3O_4/ZrO_2 nanocomposite.

The catalytic activity of the formed nanocomposites was found as the following sequence: Ag NPs/ZrO_2 > Ag/Fe_3O_4/ZrO_2 > ZrO_2 NPs > ZrO_2 NPs (550 °C) > Fe_3O_4/ZrO_2. This trend shows the amount of dye molecules adsorption on the catalyst surface and electron transfer from the BH_4^- to the pollutant since the rate-limiting step depends on the various factors such as the size of nanoparticles, structure and surface network of the catalysts (Scheme 1). The prepared Ag nanocomposites are much more reactive than unmodified ZrO_2 NPs and Fe_3O_4/ZrO_2 with Ag NPs, because the electron transfer process takes place on the Ag NPs surface [51]. In this study, ZrO_2 NPs or Fe_3O_4/ZrO_2 as supports prevents the Ag NPs aggregation in the reaction mixture, this leads to higher activity of the synthesized catalysts. The magnetically recoverable Ag/Fe_3O_4/ZrO_2 has better catalytic activity in the reduction process of pollutants than previously reported catalysts in literature [52-54].

3.4. Investigation of catalyst recyclability

At the end of reduction reaction, the Ag/Fe_3O_4/ZrO_2 catalyst was removed from reaction suspension using an external magnetic field, washed with distilled water and dried in the furnace at 80 °C. The recyclability and stability of the recovered Ag/Fe_3O_4/ZrO_2 catalyst were evaluated in the reduction of MO on the same conditions explained in the section 2.7. The catalyst was reused in further 3 cycles and the reaction times were 7.5, 8 and 8 min after one, two and three catalytic runs, respectively. No significant decrease in the reduction times confirms good stability of the formed nanocomposite under the reaction conditions.

4. Conclusions

In this investigation, successful preparation of ZrO_2 NPs and ZrO_2/Fe_3O_4 nanocomposite was performed via sol-gel and co-precipitation methods. The aqueous *C. cyanus* flower extract was used for the reduction of

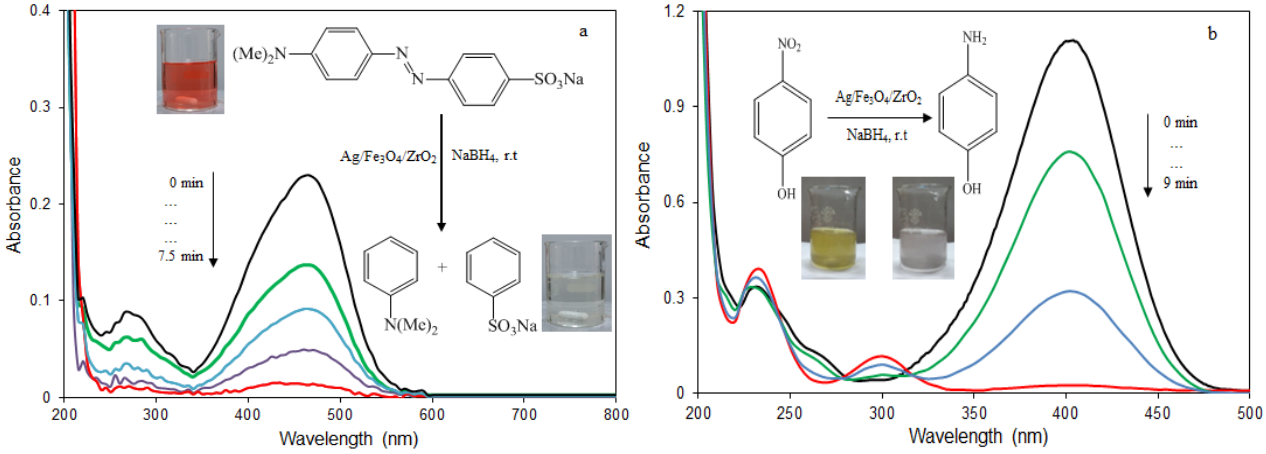

Fig. 8. UV-vis spectra of reduction process for MO (a) and 4-NP (b) in the presence of $Ag/Fe_3O_4/ZrO_2$ nanocomposite (3 mg) at several intervals: dye concentration 3×10^{-5} M (MO) and 2.5×10^{-3} M (4-NP), $NaBH_4$ concentration 5.3×10^{-3} M (MO) and 88×10^{-3} M (4-NP).

Table 1. Reaction times for the reduction of MO (3×10^{-5} M) and 4-NP (2.5×10^{-3} M) in different conditions at room temperature.

Compound	$[NaBH_4]$ (M)	Catalyst (mg)	Time (min)
MO	5.3×10^{-3}	-	65
	5.3×10^{-3}	ZrO_2 (3)	25
	5.3×10^{-3}	ZrO_2 annealed at 550 °C (3)	33.5
	-	Ag/ZrO_2 (3)	120[a]
	5.3×10^{-3}	Ag/ZrO_2 (3)	5
	5.3×10^{-3}	Ag/ZrO_2 (6)	4
	5.3×10^{-3}	Fe_3O_4/ZrO_2 (3)	37
	5.3×10^{-3}	$Ag/Fe_3O_4/ZrO_2$ (3)	7.5
	5.3×10^{-3}	$Ag/Fe_3O_4/ZrO_2$ (6)	5.5
4-NP	4.4×10^{-2}	-	100
	4.4×10^{-2}	ZrO_2 (3)	35.5
	-	Ag/ZrO_2 (3)	120[a]
	4.4×10^{-2}	Ag/ZrO_2 (3)	8.5
	4.4×10^{-2}	Ag/ZrO_2 (6)	6
	4.4×10^{-2}	Fe_3O_4/ZrO_2 (3)	50
	4.4×10^{-2}	$Ag/Fe_3O_4/ZrO_2$ (3)	16
	8.8×10^{-2}	$Ag/Fe_3O_4/ZrO_2$ (3)	9

[a]No reaction.

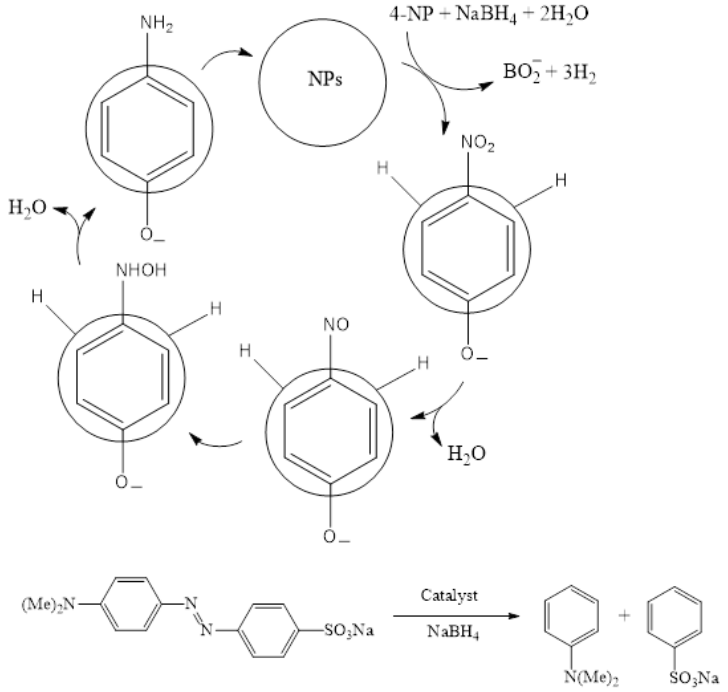

Scheme 1. Proposed mechanism for the reduction of 4-NP and MO on the catalyst surface.

silver ions and stabilization of the formed Ag NPs on the surfaces of ZrO_2 nanocomposites. The synthesized nanocomposites were characterized by different techniques and used in the reduction of MO and 4-NP at room temperature. The as-prepared $Ag/Fe_3O_4/ZrO_2$ as a magnetically recoverable and stable catalyst with high activity in the reduction process can be reused for several cycles without a significant decrease in its catalytic ability.

Acknowledgements

The authors thank University of Qom for financial support of this work.

References

[1] M. Karimi-Shamsabadi, M. Behpour, A. Kazemi Babaheidari, Z. Saberi, J. Photochem. Photobiol. A: Chem. 346 (2017) 133–143.
[2] A. Nezamzadeh-Ejhieh, S. Khorsandi, J. Ind. Eng. Chem. 20 (2014) 937–946.
[3] A. Nezamzadeh-Ejhieh, Z. Ghanbari-Mobarakeh, J. Ind. Eng. Chem. 21 (2015) 668–676.
[4] A. Nezamzadeh-Ejhieh, N. Moazzeni, J. Ind. Eng. Chem. 19 (2013) 1433–1442.
[5] A. Nezamzadeh-Ejhieh, M. Karimi-Shamsabadi, Appl. Catal. A 477 (2014) 83-92.
[6] A. Buthiyappan, A.R.A. Aziz, W.M.A.W. Daud, Rev. Chem. Eng. 32 (2016) 1–47.
[7] M. Hamadanian, A. Reisi-Vanani, A. Majedi, J. Iran. Chem. Soc. 7 (2010) Supplement 2, S52–S58.
[8] S. Tangestaninejad, M. Moghadam, V. Mirkhani, I. Mohammadpoor-Baltork, H. Salavati, J. Iran. Chem. Soc. 7(2010) Supplement 2, S161–S174.
[9] H. Pouretedal, M. Fallahgar, F. Sotoudeh Pourhasan, M. Nasiri, Iran. J. Catal. 7 (2017) 317-326.
[10] S.A. Hosseini, R. Saeedi, Iran. J. Catal. 7 (2017) 37-46.
[11] S. Dianat, Iran. J. Catal. 8 (2018) 121-132.
[12] N. Elmi Fard, R. Fazaeli, Iran. J. Catal. 8 (2018) 133-141.
[13] A. Bagheri Ghomi, V. Ashayeri, Iran. J. Catal. 2 (2012) 135-140.
[14] M.H. Habibi, E. Askari, Iran. J. Catal. 1 (2011) 41-44.
[15] M. Shekofteh-Gohari, A. Habibi-Yangjeh, Ceram. Int. 43 (2017) 3063-3071.
[16] M. Nasrollahzadeh, M. Atarod, S.M. Sajadi, Appl. Surf. Sci. 364 (2016) 636-644.
[17] A. Rostami-Vartooni, IET Nanobiotechnol. 11 (2017) 349-359.
[18] A. Nezamzadeh-Ejhieh, M. Khorsandi, Iran. J. Catal. 1 (2011) 99-104.
[19] M. Shekofteh-Gohari, A. Habibi-Yangjeh, Solid State Sci. 48 (2015) 177-185.
[20] B. Khodadadi, Iran. J. Catal. 6 (2016) 305–311.
[21] M. Nasrollahzadeh, M. Maham, A. Rostami-Vartooni, M. Bagherzadeh, S.M. Sajadi, RSC Adv. 5 (2015) 64769-64780.
[22] H. Faghihian, A. Bahranifard, Iran. J. Catal. 1 (2011) 45-50.
[23] A. Rostami-Vartooni, M. Alizadeh, M. Bagherzadeh, Beilstein J. Nanotechnol. 6 (2015) 2300-2309.
[24] B.M. Reddy, A. Khan, Cat. Rev. Sci. Eng. 47 (2005) 257-296.

[25] M. Kumar, G.B. Reddy, Phys. Status Solidi B 246 (2009) 2232-2237.
[26] J.B. Park, Nat. Prod. Res. 26 (2012) 1465-1472.
[27] P.M. Kus, I. Jerkovic, C.I.G. Tuberoso, Z. Marijanovic, F. Congiu, Food Chem. 142 (2014) 12-18.
[28] F. Riahi, M. Bagherzadeh, Z. Hadizadeh, RSC Adv. 5 (2015) 72058–72068.
[29] A. Rostami-Vartooni, M. Nasrollahzadeh, M. Alizadeh, J. Colloid Interface Sci. 470 (2016) 268-275.
[30] M. Bordbar, N. Negahdar, M. Nasrollahzadeh, Sep. Purif. Technol. 191 (2018) 295-300.
[31] M. Nasrollahzadeh, S.M. Sajadi, A. Rostami-Vartooni, M. Khalaj, J. Mol. Catal. A: Chem. 396 (2015) 31-39.
[32] B. Khodadadi, M. Bordbar, M. Nasrollahzadeh, J. Colloid Interface Sci. 490 (2017) 1-10.
[33] S.Z. Hejazi, A.F. Shojaei, K. Tabatabaeian, F. Shirini, J. Serb. Chem. Soc. 80 (2015) 971-982.
[34] H. Jiang, P. Chen, S. Luo, X. Tu, Q. Cao, M. Shu, Appl. Surf. Sci. 284 (2013) 942-949.
[35] D. Prakashbabu, R. Hari Krishna, B.M. Nagabhushana, H. Nagabhushana, C. Shivakumara, R.P.S. Chakradar, H.B. Ramalingam, S.C. Sharma, R. Chandramohan, Spectrochim. Acta Part A 122 (2014) 216-222.
[36] P. Chen, W. Zhang, M. Li, P. Ai, L. Tian, H. Jiang, RSC Adv. 6 (2016) 35859-35867.
[37] E. Karaoglu, A. Baykal, M. Senel, H. Sozeri, M.S. Toprak, Mater. Res. Bull. 47 (2012) 2480-2486.
[38] X. Feng, X. Lou, Sep. Purif. Technol. 147 (2015) 266-275.
[39] W.W. Anku, S.O.-B. Oppong, S.K. Shukla, E.S. Agorku, P.P. Govender, Prog. Nat. Sci. Mater. Int. 26 (2016) 354-361.
[40] R. Dwivedi, A. Maurya, A. Verma, R. Prasad, K.S. Bartwal, J. Alloys Compd. 509 (2011) 6848-6851.
[41] T. Tätte, M. Part, R. Talviste, K. Hanschmidt, K. Utt, U. Maeorg, I. Jogi, V. Kiisk, H. Mandar, G. Nurkb, P. Rauwel, RSC Adv. 4 (2014) 17413-17419.
[42] Z. Sherafat, I. Antunes, C. Almeida, J. R. Frade, M.H. Paydar, G.C. Matherd, D.P. Fagg, Dalton Trans. 43 (2014) 9324-9333.
[43] A. Nezamzadeh-Ejhieh, S. Tavakoli-Ghinani, C.R. Chim. 17 (2014) 49–61.
[44] Z.L. Chen, Y. Sun, P. Huang, X.P. Zhou, Nanoscale Res. Lett. 4 (2009) 400-408.
[45] X. Fu, J. Liu, X. He, Colloids Surf. A: Physicochem. Eng. Asp. 453 (2014) 101-108.
[46] A. Rostami-Vartooni, M. Nasrollahzadeh, M. Salavati-Niasari, M. Atarod, J. Alloys Compd. 689 (2016) 15-20.
[47] A. Rostami-Vartooni, M. Nasrollahzadeh, M. Alizadeh, J. Alloys Compd. 680 (2016) 309-314.
[48] S.D. Khairnar, M.R. Patil, V.S. Shrivastava, Iran. J. Catal. 8 (2018) 143-150.
[49] S. Aghdasi, M. Shokri, Iran. J. Catal. 6 (2016) 481-487.
[50] S.P. Deshmukh, R.K. Dhokale, H.M. Yadav, S.N. Achary, S.D. Delekar, App. Surface Sci. 273 (2013) 676-683.
[51] K. Hayakawa, T. Yoshimura, K. Esumi, Langmuir 19 (2003) 5517-5521.
[52] P. Deka, R.C. Deka, P. Bharali, New J. Chem. 38 (2014) 1789-1793.
[53] K.-L. Wu, R. Yu, X.-W. Wei, Cryst. Eng. Commun. 14 (2012) 7626-7632.
[54] F.-H. Lin, R.-A. Doong, J. Phys. Chem. C 115 (2011) 6591-6598.